ANTIOXIDANTS & REDOX SIGNALING
Volume 9, Number 12, 2007

DOI: 10.1089/ars.2007.1801

Forum Original Research Communication

Heme Oxygenase-1 Ameliorates Ischemia/Reperfusion Injury by Targeting Dendritic Cell Maturation and Migration

KATJA KOTSCH,[1] PAULO N. A. MARTINS,[2,5] ROMAN KLEMZ,[1] UWE JANSSEN,[3] BERNHARD GERSTMAYER,[3] ANNELIE DERNIER,[1] ANJA REUTZEL-SELKE,[2] ULRIKE KUCKELKORN,[4] STEFAN G. TULLIUS,[2,5]* and HANS-DIETER VOLK[1,6]*

ABSTRACT

Ischemia/reperfusion injury (IRI) has a major impact on short- and long-term renal allograft survival by increasing graft immunogenicity. Donor preconditioning by inducing heme oxygenase 1 (HO-1) has been proven to exert cytoprotective and antiinflammatory effects on the graft, thus resulting in reduced graft immunogenicity. The study analyzed the effects and mechanisms of HO-1–mediated cytoprotection in rat kidney transplants exposed to cold preservation. We studied the differential gene-expression patterns of allografts after either short or long cold ischemia using a customized cDNA microarray. Prolonged cold ischemia led, 12 h after engraftment, to enhanced levels of adhesion molecules, heat-shock proteins, chemokines (CXCL10), and a remarkable upregulation of immunoproteasomes. Next we addressed the question whether induction of HO-1 or its byproduct carbon monoxide (CO) in organ donors targets these candidate markers related to enhanced immunogenicity. Induction of HO-1 or CO in organ donors 24 h before organ harvesting resulted in reduced mRNA levels of immunoproteasomes, MHC class II expression, and co-stimulatory molecules in the recipient's spleen, suggesting diminished migration and activation of donor dendritic cells. This observation suggests that HO-1/CO induction protects marginal allografts by inhibiting the immunogenicity of donor-derived dendritic cells. *Antioxid. Redox Signal.* 9, 2049–2063.

INTRODUCTION

Ischemia/reperfusion injury (IRI) has a major impact on short- and long-term renal allograft survival. Historically, IRI was considered a risk factor for delayed graft function (DGF), which is a common clinical situation after kidney transplantation, associated with enhanced risk of graft loss and increased frequencies of acute rejections (22, 25, 31). Synergistically with other donor factors, such as age, hypertension, and brain death, IRI determines the pre/perioperative damage of the graft. In addition to direct toxic effects on the graft, recent data support the idea of increasing graft immunogenicity induced by IRI that amplifies alloantigen-specific processes, resulting in the development of chronic allograft nephropathy (CAN) in the long-term outcome (27, 36, 37).

With the increasing knowledge of the link between innate and adaptive immunity, particularly after the delivery of "danger" signals to pattern-recognition receptors, it is speculated that enhanced allograft immunogenicity after IRI is due to the activation of innate immunity by endogenous Toll-like receptor li-

[1]Institute of Medical Immunology, Universitätsmedizin Charité Campus Mitte, Berlin, Germany.
[2]Department of General-, Visceral- and Transplantation Surgery, Universitätsmedizin Charité Campus Virchow, Berlin, Germany.
[3]Miltenyi Biotec GmbH, MACSmolecular Business Unit, Cologne, Germany.
[4]Institute of Biochemistry, Universitätsmedizin Charité Campus Mitte, Berlin, Germany.
[5]Division of Transplant Surgery, Brigham and Women's Hospital, Harvard Medical School, Boston, Massachusetts.
[6]Berlin-Brandenburg Center for Regenerative Therapies (BCRT), Universitätsmedizin Charité Campus Virchow, Berlin, Germany.
*S.G. Tullius and H.-D. Volk contributed equally as senior authors.

gands, such as heat-shock proteins (HSPs) which trigger alloreactivity by enhanced antigen presentation (22, 24). Multiple immune processes are associated with IRI, occurring through a complex interaction between renal hemodynamics, inflammatory mediators, and endothelial and tubular injury. These processes are reflected by the recruitment of activated neutrophils and monocytes/macrophages (9, 13), altered cell-adhesion patterns (42), induction of cytokines/chemokines (4), and complement activation (6). This leads to the recruitment and activation of leukocytes, which generate reactive oxygen species (ROS) and cytokines, thus resulting in enhanced injury (7). Subsequent to IRI, the inflammatory response further results in endothelial activation with enhanced dendritic cell (DC) adhesion and migration, accompanied with the expression of MHC class II and co-stimulatory molecules, thus increasing graft immunogenicity. Activated donor DCs begin to migrate from the graft to the recipient lymphoid compartments, finding their way to both draining lymph nodes and the spleen of the recipient, finally initiating direct allorecognition. Consequently, a stronger alloresponse results in higher frequencies of acute rejection episodes and accelerated CAN.

For a better understanding of the molecular changes leading to accelerated CAN, major contributions have been made identifying dynamic changes of IRI in experimental warm ischemia models using gene-expression microarray analyses (45, 50). Recent studies also reported on gene-expression profiles after cold IRI in heart transplantation models (2, 43). Although a number of studies have focused on mechanisms of IRI in organ transplantation, early regulators and their therapeutic relevance have not been explored. In this context, the beneficial effects of heme oxygenase 1 (HO-1) activity have been proven as a promising tool in renal allograft protection. HO-1 catabolizes heme into the three byproducts: carbon monoxide (CO), iron, and biliverdin (46), and biliverdin is further converted to bilirubin through biliverdin reductase. Three isoforms of HO (HO-1, HO-2, and HO-3) have been identified. HO-1 is classified as heat-shock protein 32 (HSP32) and is induced in response to various stimuli such as hypoxia, endotoxin, heat shock, ROS, or ischemia, acting as a cytoprotective protein (32, 38). Meanwhile, extensive experimental studies demonstrated that donor preconditioning by inducing HO-1 exerts cytoprotective and antiinflammatory effects in the graft. In particular, we demonstrated that HO-1 induction by a single donor treatment with the synthetic metalloporphyrin cobalt-protoporphyrin-IX (CoPPIX) ameliorated IRI in the rat and preserved long-term function (48). Although the byproduct CO is not an antioxidant (49), it can cause induction of antioxidant genes and demonstrates antiapoptotic effects as well (33). Several reports have demonstrated that CO is able to prevent IRI or allograft rejection *via* its antiinflammatory and antiproliferative effects (3, 11, 19, 21, 33, 49). Furthermore, very recently we showed that induction of CO by applying the prodrug methylene chloride (MC) in donor animals reduces the frequencies of donor-derived DCs in the kidney graft, peripheral blood, and spleen, associated with decreased numbers of donor-reactive T cells and prevention of CAN (28). Especially the latter observation suggests that one of the major aspects of reducing graft immunogenicity after the induction of HO-1 or treatment with its byproducts might be mediated by modulating maturation or migration of DCs.

The aim of the present study was to investigate potential mechanisms of HO-1–mediated cytoprotection against nonantigenic injury in a well-defined rat model of kidney transplantation (F344–Lewis) after prolonged cold ischemia associated with accelerated CAN. In a first series of experiments, we studied the differential gene-expression pattern of allografts from F344 donors after either short (20 min) or long (24 h) cold ischemia using a customized cDNA microarray spotted with 737 immune-related genes. In a second series of experiments, we addressed the question whether induction of HO-1 or CO in organ donors would be associated with targeting identified candidate markers. In summary, our data suggest that HO-1 or CO induction inhibits donor DC maturation and activation, resulting in reduced trafficking to secondary lymphoid organs, thus leading to reduced immunogenicity and antidonor reactivity.

MATERIAL AND METHODS

Animal model and operative techniques

A well-established model for renal allograft deterioration was used. Inbred adult (200–250 g body weight) male Fisher (F344) and Lewis (LEW) rats (Harlan Winkelmann, Borchen, Germany) served as donors and recipients, respectively. Renal allografts from F344 donors were transplanted into LEW recipients using standard microsurgical techniques. All animals were anaesthetized with pentobarbital, 30 mg/kg (Nembutal Sodium Solution; Abbott Laboratories, Chicago, IL).

Experimental groups

For the microarray experiment, grafts were perfused with University of Wisconsin (UW) solution at 4°C, undergoing 20 min. ($n = 3$) or 24 h of cold ischemia ($n = 3$). Engrafted organs were removed after 12 h. For the pretreatment study, donor animals were either treated with methylene chloride (MC, CH_2Cl_2, 100 mg/kg, p.o; Sigma Aldrich, Munich, Germany), or CoPPIX (5 mg/kg, i.p.; Porphyrin Products, Inc., Logan, UT) 24 h before organ harvesting or remained untreated ($n = 6$). Grafts were also perfused with UW solution at 4°C and stored for 6 h at 4°C. Removed organs after 12 h of engraftment were transferred immediately in liquid nitrogen and stored at −80°C until total RNA extraction. Untreated normal kidneys from F344 rats served as controls. Animal experiments were performed with the written permission of the local authorities (Landesamt für Gesundheitsschutz, Arbeitsschutz und Technische Sicherheit, Berlin, Germany).

Histology

Tissue samples were fixed in 4% buffered formalin and embedded in paraffin. Hematoxylin-eosin (H&E) stains were evaluated by light microsocopy under the supervision of an experienced pathologist.

cDNA microarray production

A customized PIQOR cDNA microarray (Miltenyi Biotec GmbH, MACSmolecular Business Unit, Cologne, Germany)

spotted with 737 rat immune-related target genes was used for analysis. Array production was done as previously described (8). In brief, defined 200- to 400-bp fragments of selected cDNAs were generated by RT-PCR (Superscript II; Invitrogen, Groningen, The Netherlands), cloned into pGEM-T Vector (Promega, Mannheim, Germany) and sequence verified. Amplified inserts (Taq PCR Master Mix; Qiagen, Hilden, Germany) were purified (Qiaquick 96 PCR BioRobot Kit; Qiagen), checked on an agarose gel, and spotted 4 times (0.2 ng) on pretreated glass slides (8) with a noncontact piezo-based spotting device.

Isolation of total RNA, labeling, and hybridization

Whole kidney tissues were disrupted with an Ultraturrax homogenizer (Janke & Kunkel, Staufen, Germany). Total RNA was extracted using the NucleoSpin RNA L Kit (Macherey-Nagel GmbH und Co KG, Düren, Germany). Sample quality and quantity were assessed with an Agilent 2100 Bioanalyzer (Agilent Technologies, Palo Alto, CA). All samples possessed 18S and 28S rRNA peaks with no RNA degradation. mRNA isolation and fluorescent labeling of the probes were performed as previously described (8). In brief, 100 μg of total RNA was combined with a control RNA consisting of an *in vitro* transcribed *Escherichia coli* genomic DNA fragment carrying a 30-nt poly(A)$^+$-tail, and the mRNA was isolated (Oligotex mRNA Mini Kit; Qiagen). The resulting mRNA was diluted in 17 μl and combined with 2 μl of a second control RNA, a mixture of three different transcripts. The mRNA was then reverse-transcribed by adding a mix consisting of 8 μl 5× First Strand Buffer (Invitrogen, Karlsruhe, Germany), 2 μl Primer-Mix (oligo-dT and randomers, 2 μl low C dNTPs (10 m*M* dATP, 10 m*M* dGTP, 10 m*M* dTTP; 4 m*M* dCTP), 2 μl FluoroLink Cy3/5-dCTP (Amersham Pharmacia Biotech, Freiburg, Germany), 4 μl 0.1 *M* DTT, and 1 μl RNasin (20-40 U) (Promega, Mannheim, Germany). 200 U of Super Script II Reverse Transcriptase (Invitrogen) was added, incubated at 42°C for 30 min, followed by the addition of a further 1 μl of Super Script II Reverse Transcriptase and incubated under the same conditions as described earlier. Then 0.5 μl of RNaseH (Invitrogen) was added and incubated at 37°C for 20 min. Cy3- and Cy5-labeled samples were combined and cleaned using QIAquick (Qiagen). Eluates were diluted in 50 μl, and 50 μl of 2× hybridization solution (Miltenyi Biotec GmbH) prewarmed to 42°C was added. Hybridization was performed according to manufacturer's guidelines (Miltenyi Biotec GmbH) using a GeneTAC hybridization station (Perkin Elmer, Langen, Germany). Then 100 μl of prehybridization solution was added, and slides were prehybridized at 65°C for 30 min. Thereafter, 100 µl purified, mixed Cy3- and Cy5-labeled probes in 2× hybridization solution was pipetted onto the slides, thereby displacing the prehybridization solution. Hybridization was then performed for 14 h at 65°C, followed by four washing steps carried out at 50°C (see also instruction manual, Miltenyi Biotec GmbH). RNA from control (nontransplanted) F344 kidneys was labeled with Cy3-dCTP, and RNA from transplanted kidneys was labeled with Cy5-dCTP.

Microarray data analysis

Image capture and signal quantification of hybridized PIQOR cDNA arrays were done with the ScanArray3000 (GSI Lumonics, Watertown, MA) and ImaGene software version 4.1 (BioDiscovery, Los Angeles, CA). For each spot, the local signal was measured inside a fixed circle of 350 μm diameter, and the background was measured outside the circle within specified rings 40 μm distant from the signal and 40 µm wide. Signal and background were taken to be the average of pixels between defined low and high percentages of maximal intensity, with percentage parameter settings for low/high being 0/97% for signal and 0/80% for background. Local background was subtracted from the signal to obtain the net signal intensity and the ratio of Cy5 to Cy3. The ratios were normalized to the median of all ratios using only those spots for which the fluorescent intensity in one of the two channels was twice the negative control. Subsequently, the mean of the ratios of four corresponding spots representing the same cDNA was computed. The negative control for each array was computed as the mean of the signal intensity of four spots representing herring sperm and four spots representing spotting buffer only. Only genes displaying a net signal intensity twofold higher in the control or treatment sample than in the negative control were used for further analysis. For linear scaling, ratios with values <1 were treated in the following way: (1/ration) x –1. Therefore, -1 and $+1$ values are considered equal. The data discussed in this publication have been deposited in NCBIs Gene Expression Omnibus (GEO, *http://www.ncbi.nlm.nih.gov/geo/*) and are accessible through GEO Series accession number GSE4441 (5, 14). All labelled samples were hybridized to PIQOR cDNA microarrays. One microarray experiment was carried out for each animal.

Cell preparation, culture, and treatments

Rat bone marrow–derived DCs (BMDCs) were obtained by culturing bone marrow cells in medium supplemented with recombinant rat IL-4 or granulocyte–macrophage colony-stimulating factor (GM-CSF) (final concentration of 4 and 1.5 ng/ml of each cytokine, respectively; Peprotech Inc., Rocky Hill, NJ). Cultures were fed with GM-CSF and IL-4 on days 3 and 6. At day 8, adherent immature bone marrow–derived DCs were used. Immature DCs were pulsed for 2 h with 50 μM CoPP. The cells were then washed twice and cultured for 16 h. DCs treated with CoPP were then cultured for a further 24 h with LPS (1 μg/ml, *Escherichia coli* 026:B6; Sigma Aldrich), and nonadherent mature DCs were collected for analysis.

Quantitative real-time RT-PCR

Real-time reverse transcriptase polymerase chain reaction (RT-PCR) was performed as described elsewhere (40). In brief, the expression of selected candidate genes was analyzed by real-time PCR using the ABI PRISM 7500 Sequence Detection System (TaqMan; Applied Biosystems, Darmstadt, Germany). All primers were designed using Primer Express software (Applied Biosystems) and validated at the Institute of Medical Immunology, Universitätsmedizin Charité. The amplification primers were designed to span the exon borders to exclude crossreac-

tivity with genomic DNA. The PCR reaction was performed in a final volume of 25 μl containing 1 μl cDNA, 12.5 μl Master Mix (TaqMan Universal PCR Master Mix; Applied Biosystems), 1 μl fluorogenic hybridization probe, 6 μl primer mix, and 5.5 μl distilled water. The amplification took place in a two-step PCR (40 cycles; 15-sec denaturation step at 95°C, and 1-min annealing/extension step at 60°C). Specific gene expression was normalized to the housekeeping gene β-actin given by the formula $2^{-\Delta Ct}$, which also showed no regulation in the microarray experiments. The result for the relative gene expression was calculated by the $2^{-\Delta\Delta}$Ct method. The mean Ct values for the genes of interest and β-actin were calculated from double determinations. Samples were considered negative if the Ct values exceeded 40 cycles.

Western blot analysis

To validate the heightened gene expression of the different immunoproteasome subunits and the immune activator PA28 subunits as a consequence of prolonged cold ischemia, Western blot analysis was performed using whole tissue lysates from rat kidneys or lysates from DCs. Tissues or cells were homogenized in protein extraction buffer (50 m*M* Tris · HCl, pH 7.4, 50 m*M* NaCl, 5 m*M* $MgCl_2$, 0.1 % Triton X-100), supplemented with complete protease inhibitor cocktail (Roche, Mannheim, Germany) using an Ultraturrax tissue homogenizer (Jahnke and Kunkel, Staufen i. Breisgau, Germany). After centrifugation (30 min., 4°C), total protein was quantified by applying Coomassie Protein Assay Kit (Perbio Science, Bonn, Germany). Aliquots of 150 μg were supplemented with 1× sample buffer and applied to a 15% SDS-PAGE. The gels were blotted onto nitrocellulose membrane, and proteins were visualized with Ponceau red staining. Blots were blocked for 1 h in blocking buffer [PBS + 5% (wt/vol) low-fat dry milk + 1% Tween 20] at room temperature and agitated overnight at 4°C in a 2,000-fold dilution of rabbit polyclonal anti-mouse MECL-1 (PSMB10), 2,000-fold dilution of rabbit polyclonal anti-mouse LPM7 (PSMB8), 1,000-fold dilution of rabbit polyclonal anti-mouse LPM2 (PSMB9), 2,000-fold dilution of rabbit polyclonal anti-mouse PA28α, and 2,000-fold dilution of rabbit polyclonal anti-mouse PA28β in blocking buffer. Antibodies were cross-reactive with rat. Blots were washed 3 times in PBS + 1% Tween 20 and incubated for 1 h in a 5,000-fold dilution of goat anti-rabbit IgG-peroxidase conjugate (Amersham Biosciences, Freiburg, Germany) in blocking buffer. After four washes, proteins were visualized on films by enhanced chemiluminescence reaction. An anti-mouse p38 MAPK monoclonal antibody (Becton Dickinson, Heidelberg, Germany) was used as loading control.

Statistics

The full data set consisting of 737 genes was used for data processing. Hierarchic clustering was performed by applying average linking clustering with the Cluster software described in Eisen *et al*. (15; *http://rana.lblgov/EisenSoftware.htm*). Statistical significance of gene expression was analyzed using t tests of unpaired data and the computer software SAM (Significance Analysis of Microarrays; SAM; *http://www-stat-class.stanford.edu/SAM/SAMservlet*). Statistical significance for gene expression assessed by real-time RT-PCR was ascertained by applying the Mann–Whitney *U* test. Differences were considered significant at $p < 0.05$.

RESULTS

Graft morphology

F344 kidney transplants that experienced either 20 min or 24 h of cold ischemia were examined 12 h after engraftment into LEW recipient rats. Twelve hours after engraftment, an increase of cellular infiltrates, tubular atrophy, and arteriosclerosis was observed in grafts after 24 h of cold ischemia compared with those subjected to 20 min of cold ischemia (Fig. 1).

cDNA Microarray hybridizations

The cDNA microarray experiment was carried out in triplicate for three individual animals of both groups. Unfortunately, the hybridization of one cDNA microarray (24 h cold ischemia) did not pass the quality control, because overall signal intensities were very low. Consequently, this array was excluded from analysis. Hierarchic clustering of grafts subjected either to 20 min or 24 h of cold ischemia illustrated clearly two distinguishable groups based on their molecular-expression pattern. Figure 2 illustrates two nodes of the dendogram showing nine induced genes.

Gene expression in kidney transplants after short-term cold ischemia

The cDNA microarray analysis revealed the expression of 87 differentially regulated genes (47 genes upregulated, twofold or more; 40 genes downregulated, twofold or more) in kidneys subjected to 20 min of cold ischemia after 12 h of engraftment compared with nontransplanted F344 control kidneys. Among the early regulated genes, the small inducible cytokine A19 (CCL19, 5.2-fold up), tissue inhibitor of metalloproteinase 1 (TIMP-1, 5.7-fold up), and the suppressor of cytokine signaling 3 (SOCS3, 5.6-fold up) represented the most strongly (more than fivefold) induced genes, whereas the transcription factor c-fos displayed the most significantly downregulated gene (c-fos, −3.7-fold down). A summary of genes that were detected in at least all three independent experiments are displayed in Table 1.

Gene expression in kidney transplants after long-term cold ischemia

As expected, the expression pattern was significantly altered after 24 h of cold ischemia, comprising 79 upregulated genes and 62 downregulated genes in kidneys derived from animals killed 12 h after engraftment compared with nontransplanted controls. Among 79 induced genes, 20 genes were upregulated more than fivefold. The analysis demonstrated that prolonged cold ischemia leads to a further increase of TIMP-1 (22.1-fold up) or adhesion molecules including intracellular adhesion molecule 1 (ICAM-1, 9.9-fold up) (see Table 1). In addition, the interferon-γ–induced chemokine 10 (IP-10, CXCL10) displayed a strong induction as

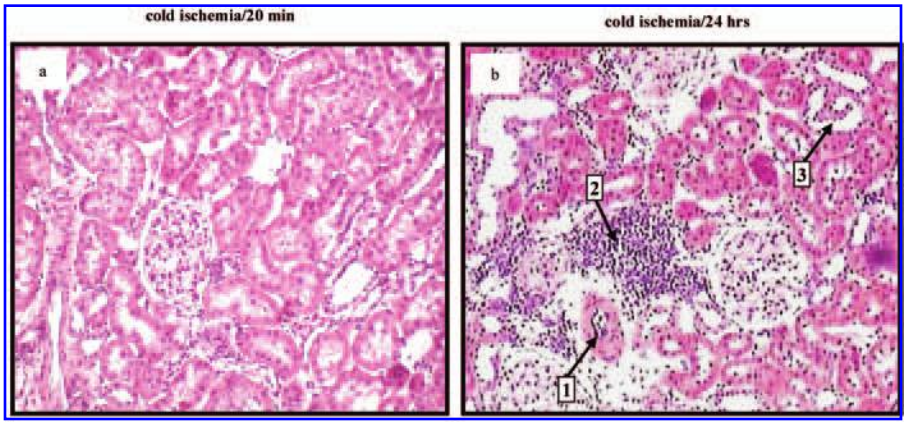

FIG. 1. Structural changes of grafts undergoing either 20 min or 24 h of cold ischemia after 12 h of engraftment. In particular, prolonged cold ischemia of 24 h led to an increase of arteriosclerosis (1), cellular infiltrates (2), and tubular atrophy (3) in kidneys already detectable within the first 12 h after transplantation (hematoxylin-eosin staining, 200x).

a result of prolonged cold ischemia (23.3-fold up). Furthermore, we discovered the increased expression of inducible proteasome β subunits (immunoproteasomes), including proteasome component C13 (PSMB8 or LMP7, 16.11-fold up), proteasome chain 7 (PSMB9 or LMP2, 5.60-fold up), and proteasome component MECL-1 (PSMB10 or MECL, 5.96-fold up). Moreover, an elevated expression for both subunits of the proteasome activator PA28α and β (PSME1, PSME2; 3.30-fold up and 3.75-fold up, respectively) could be observed (see Table 1). In contrast, no differential expression of the constitutively expressed proteasome β subunits X, Y, and Z (PSMB5, PSMB6, and PSMB7) could be detected (data not shown). For further confirmation of the gene-expression data obtained by cDNA microarrays, we verified the gene expression by real-time RT-PCR. Figure 3 illustrates the results obtained for the candidate markers IP-10, ICAM-1, CCL19, LMP2, LMP7, and MECL-1.

Enhanced immunoproteasome induction in kidney grafts underlying prolonged cold ischemia

To clarify whether increased expression of inducible immunoproteasomes is also observed at the protein level, we examined the expression of LMP2, LMP7, MECL-1, and PA28α/β by Western blot analysis. Figure 4 demonstrates the upregulation of LMP2 (PSMB9) and LMP7 (PSMB8) at the protein level in grafts underlying 24 h of cold ischemia compared with native kidneys or grafts undergoing a short cold-ischemia time. Although we detected a more than threefold induction of the proteasome activator PA28α and PA28β subunits at the mRNA level (see Fig. 1), these were barely induced at the protein level. Unfortunately, we did not succeed in detecting MECL-1 (PSMB10) by Western blot analysis, as available antibodies have been nonreactive. Consequently, we proceeded to analyze the different immunoproteasome subunits by real-time RT-PCR.

Donor pretreatment with CoPP or MC did not inhibit ischemia/reperfusion injury–induced immunoproteasome induction in the graft

The induction of HO-1 or the treatment with its byproducts has been demonstrated to exert cytoprotective and antiinflammatory effects in various transplantation models (21–29). To ascertain whether donor pretreatment with CoPP or MC targets

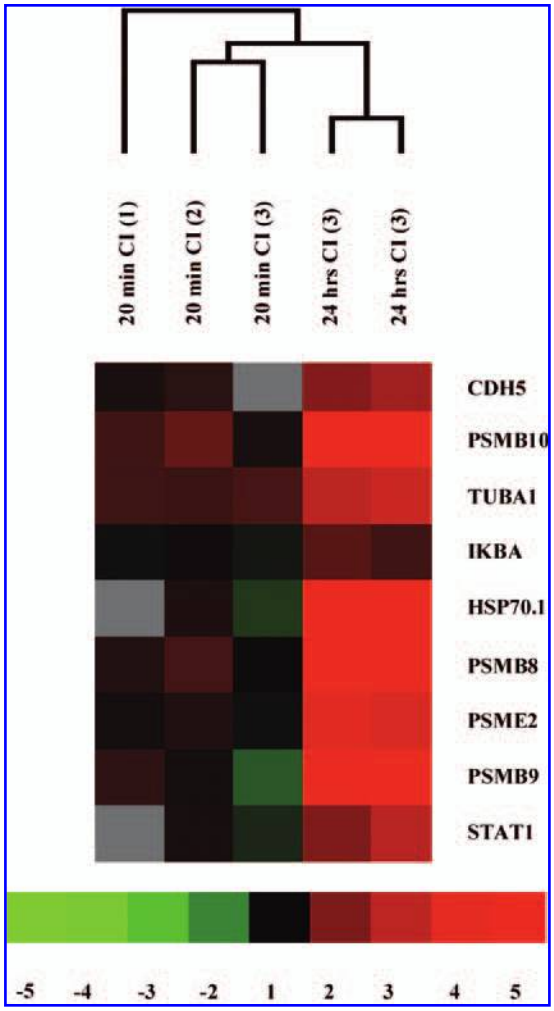

FIG. 2. Gene-expression dendogram showing hierarchic clustering of nine induced genes affected during IRI in rat kidneys undergoing either 20 min or 24 h of cold ischemia after an observation period of 12 h. Among the highly induced genes, the inducible immunoproteasome subunits LMP2 (PSMB9), LMP7 (PSMB8), and MECL-1 (PSMB10) were uncovered. CDH5, vascular endothelial–cadherin precursor; HSP, heat-shock protein; IκBa, I-kappa-B alpha; PSME2, 11S proteasome regulator PA28 β subunit; STAT1, signal transducer and activator of transcription 1 a/β; TUBA1, tubulin α-1 chain.

TABLE 1. TRANSCRIPTS INDUCED AFTER SHORT AND PROLONGED COLD ISCHEMIA IN RENAL ALLOGRAFTS

Gene name	*Gene symbol*	*UniGene ID*	*Duration of cold ischemia*	
			20 min	*24 h*
Apoptosis related				
Tissue inhibitor of metalloproteinase 1	TIMP1	Rn.25754	+5.67	+22.12
Tumor necrosis factor receptor	TNFR1	Rn.11119	+2.56	+2.28
Tumor necrosis factor ligand superfamily ligand 13	APRIL	Rn.19955	+2.20	−2.56
BCL2/Adenovirus E1B 19-kDa protein-interacting protein 3	BNIP3	Rn.2060	−1.28	−3.22
Cellular tumor antigen p53	p53	Rn.54443	+1.50	+5.21
Secreted apoptosis related protein	SARP2	Rn.19802	+2.05	+2.87
TNF-related weak inducer of apoptosis	TNFSF12	Rn.3211	−1.58	−4.34
RAS-related protein (p23)	RRAS	Rn.14692	+1.61	+1.88
Clusterin	CLU	Rn.1780	+3.51	+13.96
Complement system				
Complement CS1 component	C1S	Rn.4037	+1.27	+2.44
Complement C4	C4A	Rn.30176	+1.85	+1.22
Cell adhesion and cytoskeleton				
Intracellular adhesion molecule 1	ICAM1	Rn.12	+3.71	+9.85
Integrin alpha 5	ITGA5	Rn.12138	+2.38	+6.67
Tubulin alpha 1 chain	TUBA	Rn.54749	+1.46	+3.11
Endoglin	ENG	Rn.12225	+1.39	+1.58
Integrin beta 1	ITGB1	Rn.25733	+1.43	+2.35
Membrane glycoprotein (SFA-1)	CD151	Rn.1465	+1.39	+1.59
Antigen presentation				
Proteasome component C13, LMP7	PSMB8	Rn.29244	−1.03	+16.11
Proteasome chain 7, LMP2	PSMB9	Rn.13686	−1.58	+5.60
Proteasome component MECL-1	PSMB10	Rn.24968	+1.45	+5.97
11S Proteasome regulator PA28 alpha subunit	PSME1	Rn.2742	+1.14	+3.30
11S Proteasome regulator PA28 beta subunit	PSME2	Rn.4017	+1.09	+3.75
Ubiquitin carboxyl-terminal hydrolase 2	USP2	Rn.19491	−1.20	ND
Metabolism				
Phosphatidylinositol 3-kinase	PIK3R1	Rn.10599	+2.24	+2.89
Alanyl (membrane) aminopeptidase	ANPEP	Rn.1132	−1.33	−7.14
Microsomal glutathione *S*-transferase	MGST3	Rn.1916	+1.18	−2.77
Superoxide dismutase	SOD1	Rn.6059	−1.21	−2.56
Immune cell infiltration				
CD68 Antigen macrosialin	CD68	Rn.12478	ND	+14.56
Receptor expression				
Colony-stimulating factor 2 receptor	CSF2RB	Rn.42930	−1.33	−7.69
Insulin-like growth factor II receptor	MPRI	Rn.270	+1.14	−2.56
Parathyroid hormone–related peptide receptor	PTHR1	Mm.3542	−1.40	−7.40
Cytokines/Chemokines				
Transforming growth factor beta	TGFb	Rn.40136	+3.46	+3.11
Chemokine (C-X-C motif) ligand 10	CXCL10	Rn.0584	+2.55	+23.27
Small inducible cytokine A19	CCL19	Rn.12445	+5.19	ND
Neurotrophin 1 (gp130 family)	CLC	Mm. 34791	+3.82	+4.76
Signaling/Transcription				
Activating transcription factor 3	ATF3	Rn.9664	+2.08	+5.94
Early growth response 1	EGR1	Rn.9096	−1.96	−3.22
p55-c-fos proto-oncogene protein	C-FOS	Rn.21076	−3.7	−5.26
Transcription factor HES1	HES-1	Rn.19727	−1.96	−3.57
B-Lymphocyte activation marker (BLAST-1)	CD48	Rn.3705	−1.34	+1.61
B-cell lymphoma 3–encoded protein	BCL3	Rn.64776	+4.43	+5.23
Nuclear factor kappa-B inhibitor	IKBA	Rn.12550	−1.03	+1.55
MAFB/Kreisler basic region/leucine zipper transcription factor	MAF1	Rn.10725	+1.29	+2.98
Suppressor of cytokine signaling 3	SOCS3	Rn.29984	+5.55	+7.30
Signal transducer and activator of transcription 1-alpha/beta	STAT1	Rn.12592	−1.03	+2.47
Signal transducer and activator of transcription 3	STAT3	Rn.10247	+1.58	+1.45
Stress-related heat-shock protein				
Heat-shock protein 105kD	HSP105	Rn.37906	−1.75	+3.3
Heat-shock protein 70kD	HSP70.1	Rn.1950	−1.04	+9.74
Heat-shock protein HSP90 alpha	HSPCA	Rn.3277	−1.11	+3.76
Coagulation cascade/Angogenesis related				
Plasminogen activator inhibitor	PAI	Rn.6169	+1.36	+8.35

IRI-associated candidate markers related to "immunogenicity" uncovered after extended cold ischemia of 24 h, we applied the same rat model by choosing a more appropriate prolonged cold ischemia time of 6 h, as it has been shown that a cold ischemic time of 6 h is sufficient to accelerate CAN. Recent data have shown that HO-1/CO protects these grafts from accelerated chronic graft injury compared with short-ischemic organs (28, 48). Surgery and IRI led to a significant increase of HO-1 mRNA in the graft versus native controls ($p < 0.01$; Fig. 5a; $n = 6$) 12 h after Tx and pretreatment of donors with CoPP-induced HO-1 before transplantation (data not shown) still sustained 12 h after transplantation at higher levels compared with controls. Furthermore, we could confirm the elevated expression of inducible proteasome subunits LMP2/7 and MECL-1 in grafts underlying prolonged (6 h) cold ischemia compared with native kidney controls at the mRNA level as a consequence of IRI ($p < 0.05$; Fig. 5a). However, treatment with CoPP or MC did not decrease intragraft mRNA expression levels of LMP2/7 and mRNA expression of MECL-1 illustrated even a slight increase compared with control kidneys (p = NS; Fig. 5a).

Donor pre-treatment with CoPP or MC did not affect intragraft mRNA expression of co-stimulatory molecules and candidate genes involved in lymphocyte trafficking

Events related to IRI activate graft DCs, which upregulate MHC class II and co-stimulatory molecules, thus increasing graft immunogenicity. It has been shown that donor conditioning with CO results in a decrease of DCs intragraft and peripherally (28, 29). However, we could not observe significant differences for MHC class II and CD86 mRNA expression in the graft (data not shown), although the induction of HO-1 and CO in the organ donor resulted in a significant increase of CD80 mRNA levels ($p < 0.01$, data not shown). Applying cDNA microarrays, we identified upregulated levels of the chemokine CCL19 after a short ischemic time, which decreased after prolonged cold ischemia (see Table 1). Furthermore, we detected elevated levels of the chemokine IP-10, a chemoattractant for activated T cells, as well as the adhesion molecule ICAM-1. To ascertain whether HO-1 or CO induction affects expression of these candidate markers, we investigated their mRNA profiles after donor preconditioning. Whereas 6 h of prolonged cold ischemia led to a significant increase of IP-10 mRNA in the transplant, confirming the cDNA microarray data ($p < 0.05$, data not shown), treatment with CoPP or MC did not lead to a significant decrease compared with untreated controls. As expected, elevated ICAM-1 mRNA levels were detected in the graft as a consequence of prolonged cold ischemia ($p < 0.05$; data not shown), but induction of HO-1 or CO in the organ donor did not alter the expression profile. The chemokine CCL19 displayed only a slight increase after 6 h of cold ischemia, and no reduction of CCL19 mRNA was detectable in the kidney graft after donor conditioning.

Donor pretreatment with CoPP or MC affects antigenicity and migration of DCs

After engraftment, donor DCs begin to migrate from the graft to the recipient lymphoid compartments. To ascertain whether

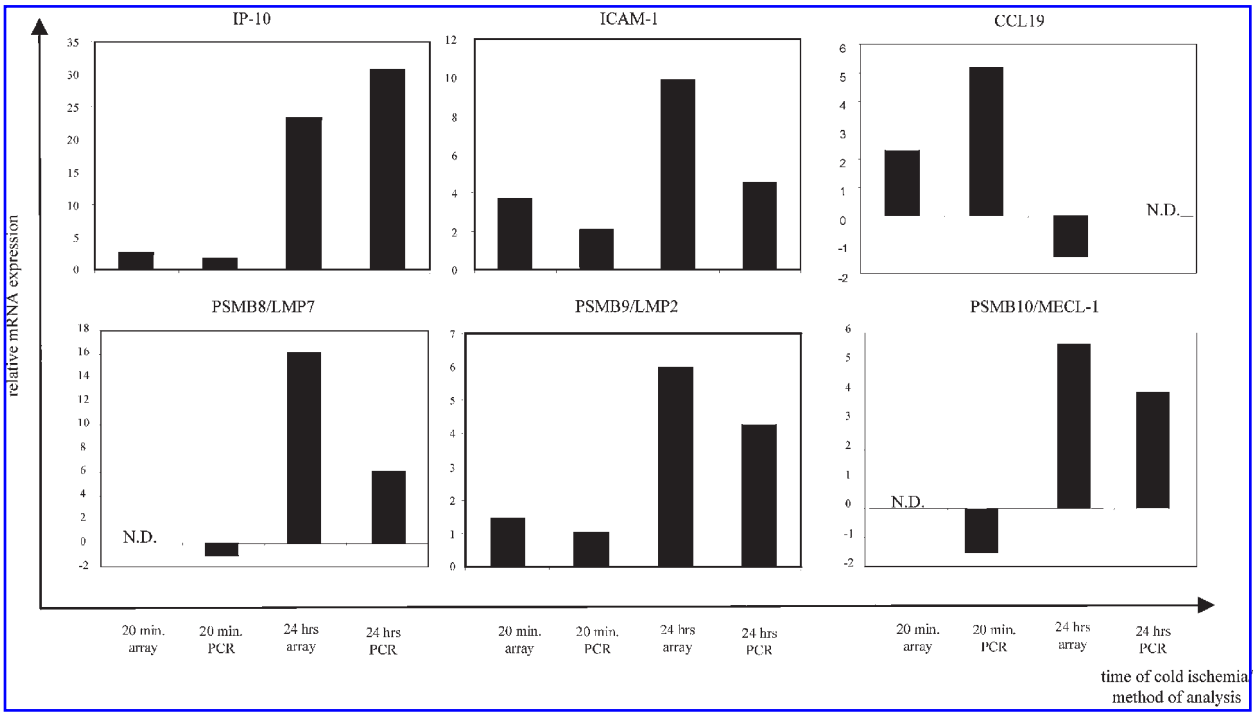

FIG. 3. Confirmation of cDNA microarray data by real-time RT-PCR. The relative mRNA expression is shown for IP-10, ICAM-1, CCL19, LMP2, LMP7, and MECL-1 compared with the expression profile gained by cDNA microarray analyzed after 12 h of engraftment. The obtained data confirmed the cDNA microarray data in the transcriptional direction ($n = 3$ animals). ND, not detected.

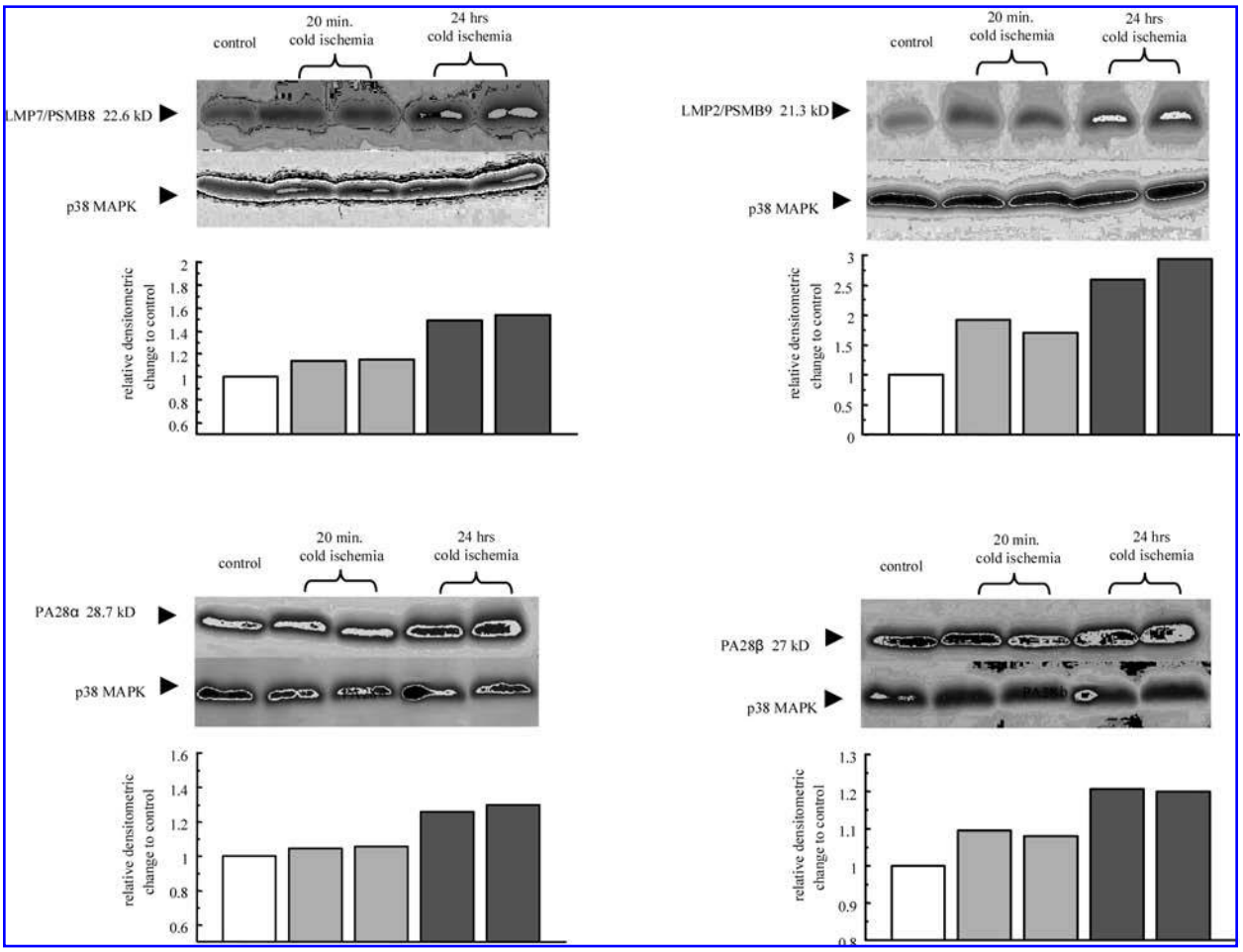

FIG. 4. Western blot analysis of the immunoproteasome subunits LMP2 (PSMB9), LMP7 (PSMB8), and the proteasome activator subunits PA28 α/β (PSME1, PSME2) in rat kidney allografts undergoing 20 min ($n = 2$) or 24 h ($n = 2$) of cold ischemia. A native F344 kidney served as control. A strong induction could be observed for both proteasome β subunits and proteasome activator subunits in kidney transplants after 24 h of cold ischemia. The staining of p38 MAPK served as internal control. Western blot analysis is representative of three independent experiments.

induction of HO-1 or CO affects migration of DCs, we investigated the recipient's spleen for the selected candidate markers. In contrast to the kidney graft, the analysis revealed significant reduced mRNA levels of all three inducible proteasome subunits selectively after CoPP and MC treatment of the kidney donor *versus* untreated controls ($p < 0.05$; Fig. 5b). Furthermore, we observed a significant decrease of MHC class II mRNA expression in the recipient's spleen (Fig. 5c), and similar effects were detected for CD80 and CD86, although the results gained for CoPP treatment displayed statistical significance only ($p < 0.05$; Fig. 5c). Whereas an induction of the chemoattractant IP-10 was detectable in the graft remaining unaffected after HO-1 or CO induction (Fig. 5c), a significant reduction of IP-10 mRNA after donor pretreatment was detected in the spleen compared with untreated controls ($p < 0.05$; Fig. 5c). In contrast, no differences for ICAM-1 mRNA expression were observed. However, in the spleen, IRI resulted in heightened CCL19 mRNA expression levels and HO-1, and CO induction abrogated this induction ($p < 0.05$; Fig. 5c).

Pretreatment with CoPP abrogates LPS-induced maturation of dendritic cells

We assumed that diminished migration of DCs to lymphoid organs is further reflected by the inhibition of maturation and therefore analyzed the effects of HO-1 induction *in vitro* using rat bone marrow–derived DCs matured with LPS. In contrast to a previous publication (12), LPS treatment alone led to a significant induction of HO-1 at the mRNA level compared with untreated DCs ($p < 0.01$; Fig. 6). This observation was further confirmed in independent experiments with murine bone marrow–derived DCs (own unpublished observations). As expected, LPS further resulted in an increase of the inducible immunoproteasome subunits LMP2/7 ($p < 0.05$; see Fig. 6) and MECL-1, although the latter did not reveal statistical significance. However, after pretreatment with CoPP for HO-1 induction, this increase was downregulated (CoPP/LPS *vs*. LPS; $p < 0.05$). CoPP treatment itself led to a decrease of MHC class II expression, but also after LPS-induced maturation, this in-

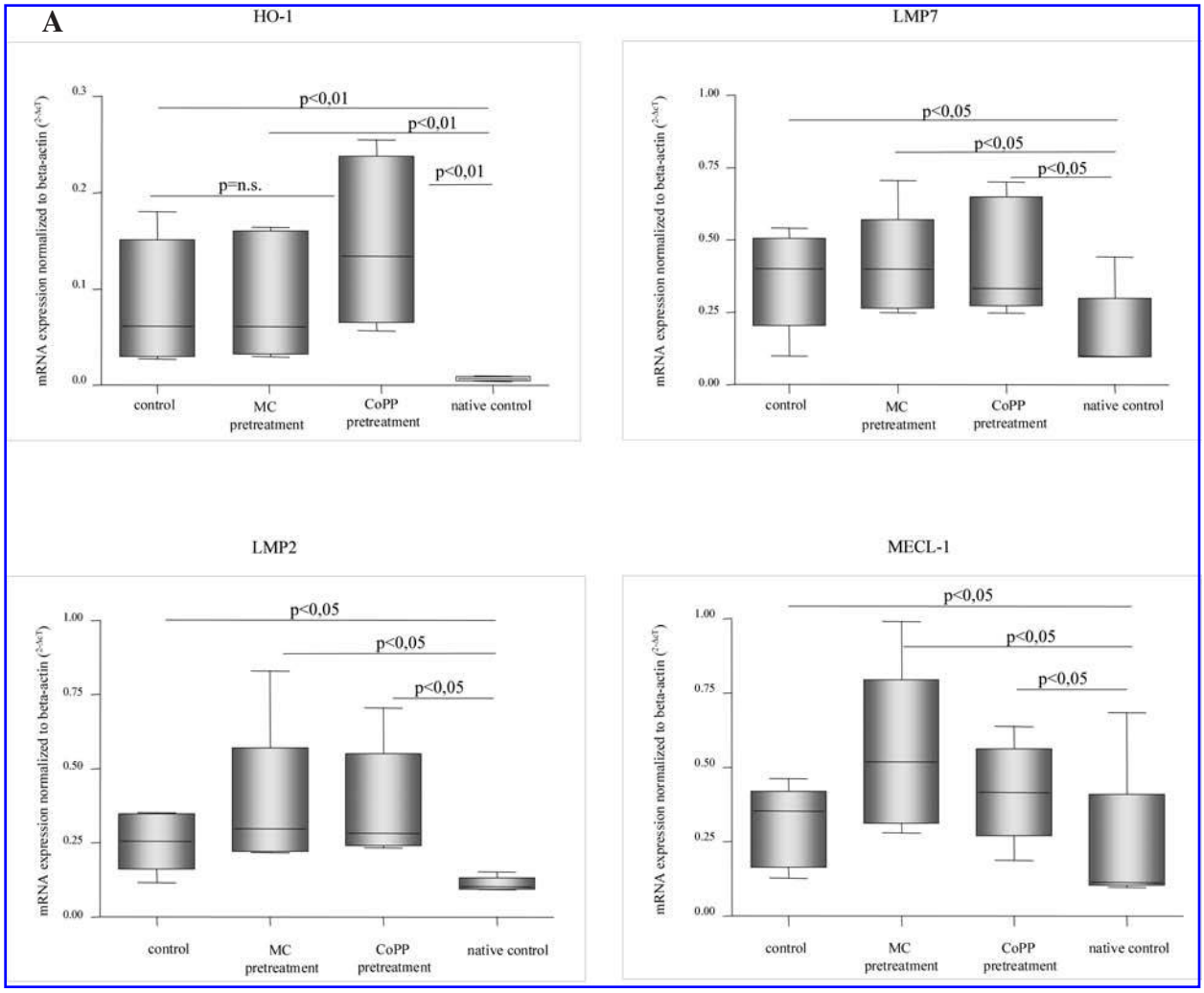

FIG. 5. Gene-expression analysis of selected markers after HO-1 and CO induction in kidney grafts and recipient's spleen. (**A**) Surgery and IRI led to a significant increase of HO-1 mRNA in the graft versus native controls 12 h after engraftment. Elevated mRNA-expression levels of the inducible proteasome subunits LMP2/7 and MECL-1 in grafts underlying cold ischemia compared with native kidney controls could be detected ($p < 0.05$). Donor treatment with CoPP (5 mg/kg, i.p.) or MC (100 mg/kg, p.o.) 24 h before harvesting did not result in a decrease of LMP2/7 and MECL-1 ($n = 6$). (**B**) In contrast to the kidney graft by investigating the recipient's spleen, the analysis revealed significant reduced mRNA levels of all three immunoproteasome subunits selectively after CoPP and MC treatment of the kidney donor *versus* untreated control ($p < 0.05$; $n = 6$). (**C**) CoPP and MC treatment led to a significant decrease of MHC class II, CD80, and CD86 mRNA expression in the recipient's spleen and a significant reduction of IP-10 mRNA after donor pretreatment was detected compared with untreated controls. No differences for ICAM-1 mRNA expression were observed. In contrast to the kidney graft, IRI increased CCL19 mRNA expression in the spleen and HO-1 as well as CO induction abrogated this induction. Box whisker plots show the 10th, 25th, 50th, 75th, and 90th percentile values of candidate markers.

crease was abrogated ($p < 0.05$; see Fig. 6). Similar observations were made for both CD80 and CD86 mRNA expression. Furthermore, we have been able to detect enhanced levels of IP-10 mRNA after inducing DC maturation with LPS, although this expression was not affected after HO-1 induction.

DISCUSSION

Although many studies described evidence for a link between enhanced IRI and inflammation, the molecular mechanisms underlying IRI and its impact on late graft outcome are still poorly understood. Therefore, we addressed the question whether cDNA microarray gene-expression analysis might reveal evidences for putative mechanisms of IRI-mediated injury. Most of the published studies investigated gene-expression profiles after IRI in experimental warm-ischemia models (45, 50) and in syngeneic cold-ischemia heart transplantation models of the mouse (2, 43). Although we analyzed only a small number of animals in an allogeneic kidney transplant model of the rat, our data generally agree with the findings of previous studies, demonstrating the induction of genes involved in the immune response (*e.g.*, CD68) (2), apoptosis (TIMP-1), and adhesion

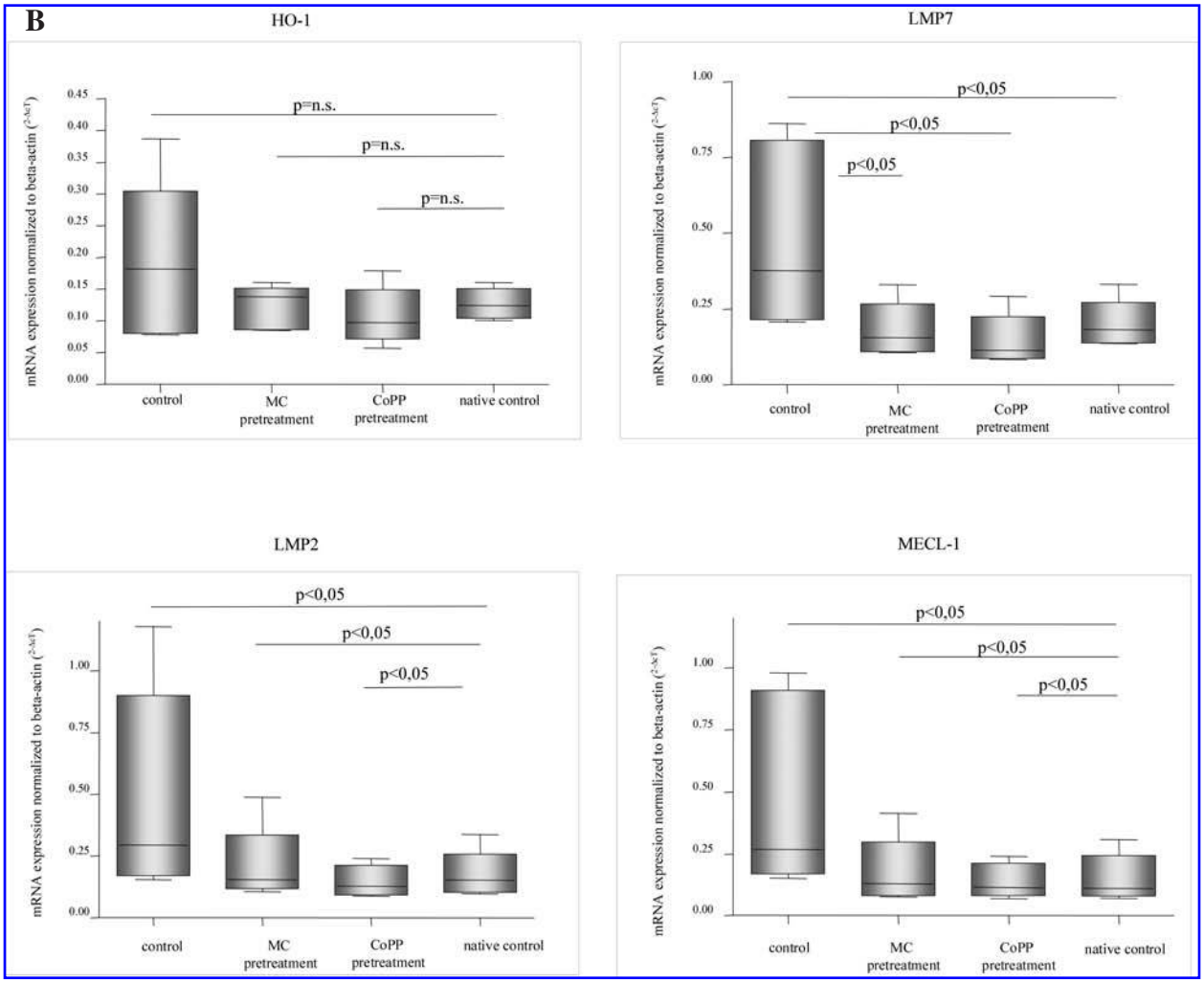

FIG. 5. *Continued.*

(*e.g.*, ICAM-1) (30) (see Table 1). Twelve hours after engraftment, our data revealed that prolonged cold ischemia is further associated with enhanced expression of HSPs (HSP105, HSP70) and the induction of chemokines, including interferon-inducible protein 10 (IP10, CXCL10) and macrophages attracting chemokines, functionally reflected by enhanced CD68 expression (see Table 1). Moreover, we provide evidence that proteasome activity is amplified in kidney transplants as a direct consequence of IRI after prolonged cold ischemia (see Figs. 2–4). The proteasome pathway plays a central role for MHC class I presentation and regulation of cell activation. Proteasomes are the main multicatalytic proteinase complex involved in stress response (*e.g.*, NF-κB activation), apoptosis, and in the generation of intracellular antigens. These antigenic peptides presented on major histocompatibility complex (MHC) class I molecules to cytotoxic T cells are generated in the cytosol by the 20S proteasome, which represents the core structure of the proteasome, made up of seven different α and β subunits each. In mammalian cells, IFN-γ leads to the induction of new proteasome β subunits LMP2 (PSMB9), LMP7 (PSMB8), and MECL-1 (PSMB10), which replace the respective constitutive catalytic subunits X (PSMB5), Y (PSMB6), and Z (PSMB7) during *de novo* assembly of proteasomes (16, 17). Furthermore, mammalian cells contain a proteasome activator called PA28 (also known as 11S regulator) composed of α and β subunits, which is likewise induced by IFN-γ but not part of the 20S proteasome itself. We uncovered the induction of all three IFN-γ–inducible proteasome subunits (LMP2, LMP7, MECL-1) and both PA28α/β subunits (PSME1 and PSME2) in grafts undergoing prolonged cold ischemia (24 h) by cDNA microarray analysis (see Table 1) and confirmed the heightened expression, with the exception of MECL-1, at the protein level (see Fig. 4). These so-called immunoproteasomes LMP2, LMP7, and MECL-1 appear to alter the cleavage profile of proteasomes, resulting in the use of specific cleavage sites, leading to the transition of generated peptides within the peptide pool (39, 41). On stimulation of cells with IFN-γ, the expression of immunoproteasomes and PA28 is induced, resulting in the enhancement of peptide degradation by the 20S proteasome or enlargement of the peptide repertoire presented to $CD8^+$

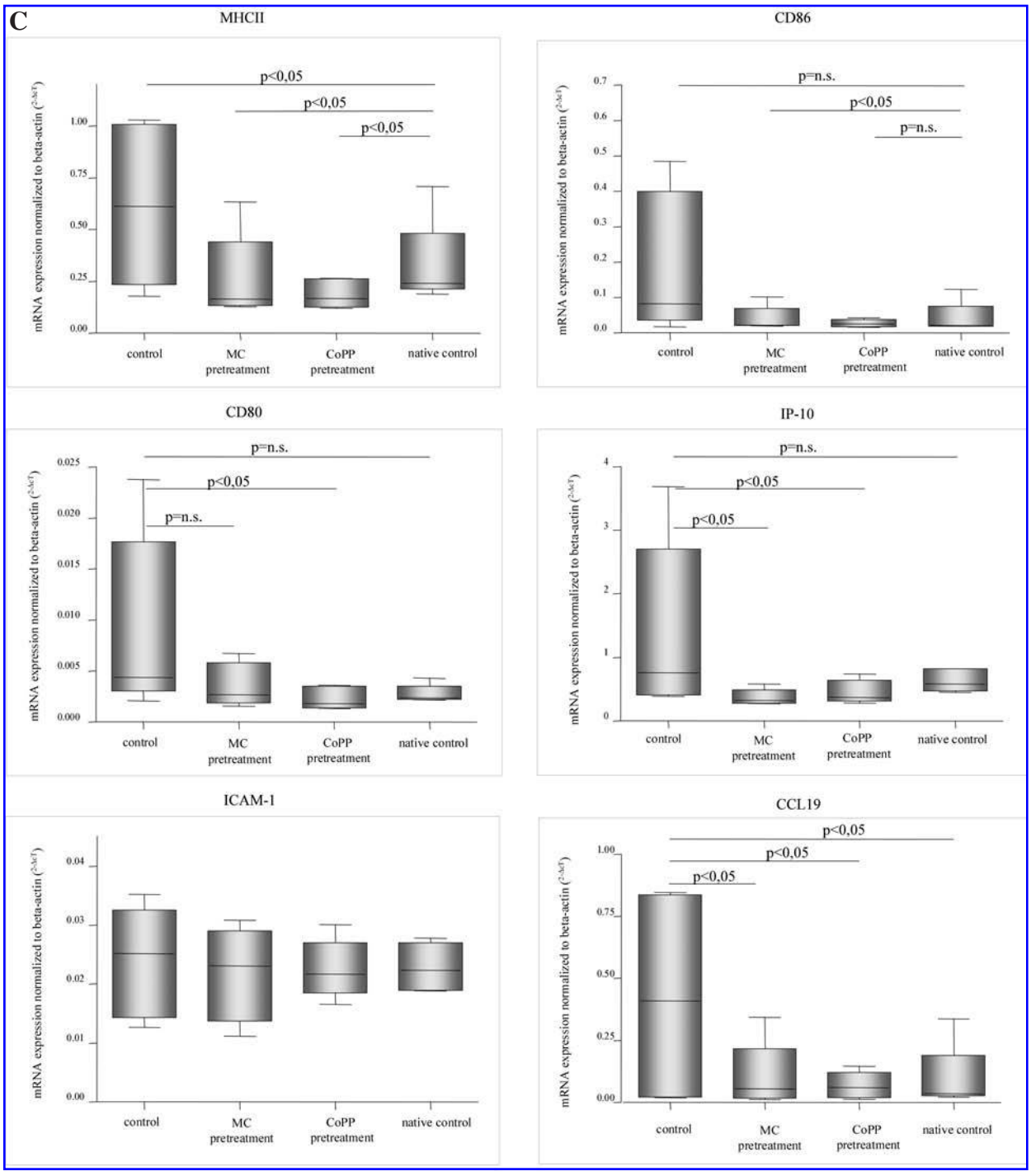

FIG. 5. *Continued.*

T cells. Furthermore, it is has been described that enhanced expression of PA28α and β in mature DCs results in PA28α/β complex formation and association with 20S proteasomes (26). This suggests a reorganization of the proteasomes, resulting in a change of antigen presentation, as PA28α/β has been demonstrated to alter polypeptide fragmentation *in vitro* (18).

Dendritic cells have the ability to capture cellular tissue antigens and present them on MHC class I molecules to Ag-specific $CD8^+$ T cells. This process, called cross-presentation, is an important pathway in controlling T-cell priming *in vivo* (1). It was shown that immature dendritic cells express similar levels of standards and immunoproteasomes (10) and that during matu-

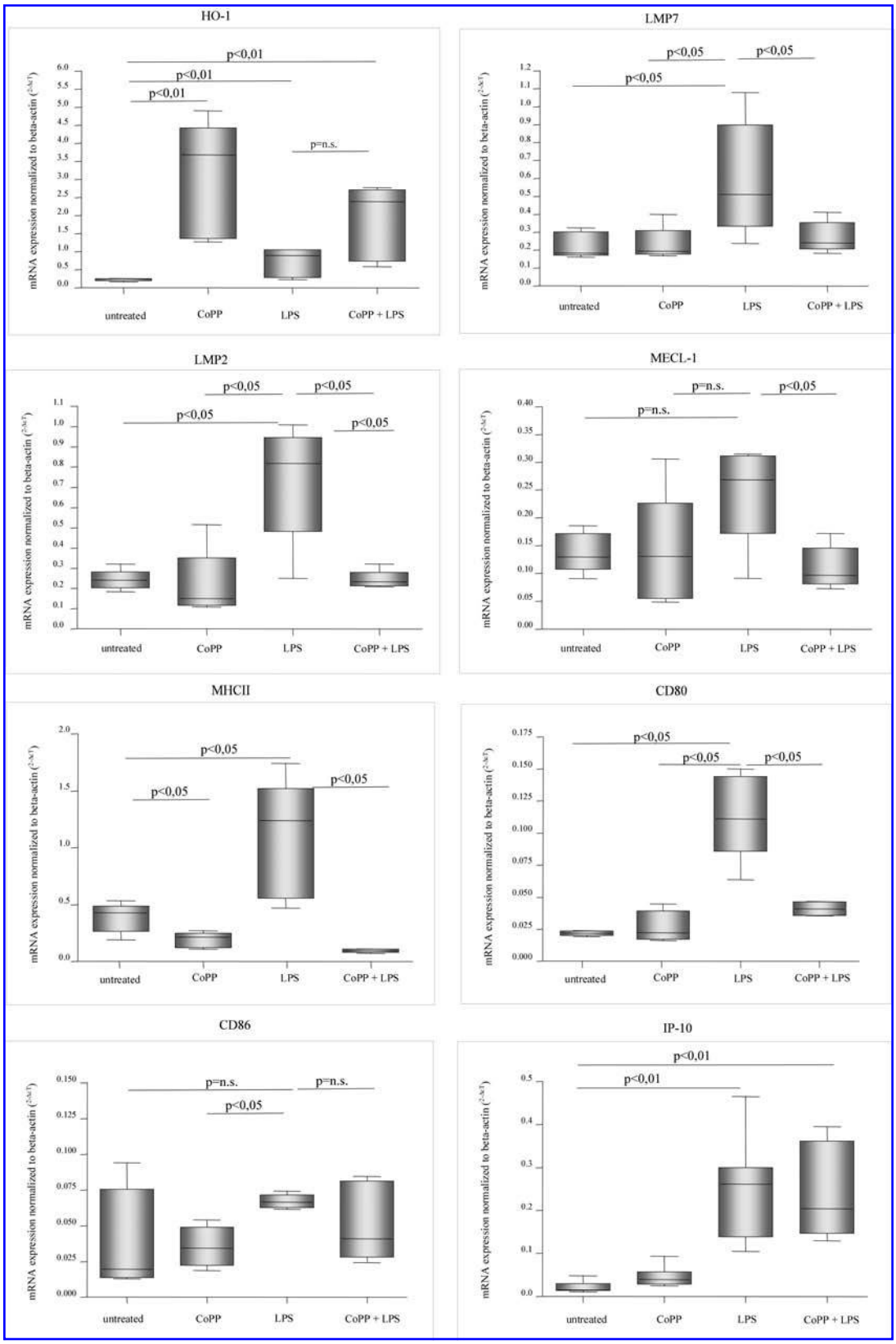

FIG. 6. Gene-expression analysis of selected markers after HO-1 induction in bone marrow–derived DCs. LPS treatment resulted in an increase of the inducible immunoproteasome subunits LMP2/7 ($p < 0.05$) and MECL-1, although the latter did not reveal statistical significance ($n = 6$). After pretreatment with CoPP (50 μmol) for HO-1 induction, this increase was downregulated (CoPP/LPS vs. LPS; $p < 0.05$). Similar observations were made for both CD80 and CD86 mRNA expression. Enhanced levels of IP-10 mRNA after inducing DC maturation with LPS were detected, although this expression was not affected after HO-1 induction. Box whisker plots show the 10th, 25th, 50th, 75th, and 90th percentile values of candidate markers.

ration, the synthesis of immunoproteasomes is stimulated. Recent data indicate that immunoproteasomes play an important role in controlling cross-priming (35) and that stimulation of TLRs leads to further induction of immunosubunits in DCs (44). It is well known that DCs play a dominant role in the early phase of alloresponse. As a consequence of graft reperfusion, and in the presence of inflammatory signals, donor-derived DCs mature and migrate to lymph nodes and spleen of the recipient. Therefore, we hypothesize that the induction of immunoproteasomes in donor graft cells after prolonged ischemic time might be one of the key events to alter allograft "immunogenicity." This might be reflected by enhanced NF-κB activation, the generation of immunoproteasomes and consequently in more-efficient generation of allogeneic T-cell epitopes [*e.g*., by antigen-presenting cells (APCs)] important for both the direct and indirect pathways presented in secondary lymphoid organs.

As HO-1 induction has emerged as a promising approach for targeting IRI, illustrated by ameliorating graft immunogenicity (28, 29, 48), we further investigated how induction of HO-1 or its byproduct CO affects uncovered target genes associated with IRI. Meanwhile, extensive studies have illustrated that donor preconditioning by inducing HO-1 improves the function of marginal organs (*e.g*., after IRI) and preserves long-term function (48). Although IRI led to a significant immunoproteasome induction in the graft, pretreatment of the kidney donor resulted in a significant downmodulation of LMP2/7 and MECL-1 mRNA in the recipient's spleen (see Fig. 5b). This decreased expression was associated with reduced MHC class II, CD80, and CD86 mRNA levels, although these effects could not be observed in the transplant. As both the induction of HO-1 and CO seem to mediate similar results, we suggest that CO, as a byproduct of HO-1 activity, may account for these effects. Lately it has been demonstrated that HO-1 induction in bone marrow–derived DCs prevents phenotypic maturation induced by LPS (12). By applying the same experimental setup, we could confirm these previous observations, illustrated by decreased mRNA expression of MHC class II, CD80, and CD86. Moreover, our experiments demonstrated that because of the maintenance of the immature phenotype of DCs, HO-1 induction resulted in a significant abrogation of immunoproteasome subunit mRNA synthesis (see Fig. 6).

A second important observation regarding altered antigen presentation after prolonged ischemia might be the affected homing of DCs by changes in the intragraft expression of C-C motif receptor 7 (CCR7) ligands. Heart allografts from $CCR7^{-/-}$ mice show a prolonged survival (20), suggesting the importance of this pathway. Indeed, we found an enhanced CCL19 expression after short ischemia compared with native kidney that, however, disappeared completely after prolonged ischemia of 24 h (see Table 1). We speculate that early intragraft downregulation of CCR7 ligands, including CCL19, results in enhanced migration of activated donor-derived APC from the graft to secondary immune organs and induces an increased alloresponse. Moderately enhanced levels of CCL19 mRNA were still detectable after 6 h of cold ischemia in the graft and more enhanced in the spleen. Interestingly, after donor pretreatment applying CoPP or MC, the induction of CCL19 as a direct consequence of IRI is diminished (see Fig. 5c), suggesting reduced DC migration. Additionally, we identified enhanced transcripts of the interferon-inducible protein 10 (IP10, CXCL10) as a direct consequence of prolonged cold ischemia (see Table 1 and Fig. 3), further emphasizing recent results reporting on IP-10 induction after of IRI in an experimental model of liver transplantation (51). However, studies of the same group illustrated in a murine model of warm ischemia that HO-1 upregulation suppressed induction of IP-10 during the course of hepatic IRI (47). This result is in line with our own data, although a suppression of IP-10 mRNA was observed only in the spleen of the recipient (see Fig. 5c). Beyond this, it has been demonstrated that DCs are able to produce substantial amounts of IP-10/CXCL10 and therefore efficiently attract $CD8^+$ T cells. Concomitantly, the elicitation of MHC class I–restricted effector functions is enhanced (34). We verified this observation in our experiments that LPS-induced inflammation resulted in enhanced levels of IP-10 mRNA in bone marrow–derived DCs; nevertheless, pretreatment with CoPP did not suppress IP-10 induction *in vitro* (see Fig. 6).

In summary, these data might help to explain the impact of a perioperative event on enhanced graft immunogenicity and how this is targeted by the induction of HO-1 or CO in the organ donor. Our data are in line with recent reports, illustrating that induction of HO-1 resulted in an inhibition of DC maturation (12) and reduced frequencies of donor-derived DCs accompanied with decreased T-cell alloreactivity in an experimental model of kidney transplantation (28). However, applying our experimental conditions, we observed, after HO-1 or CO induction in the organ donor, significant changes of maturation-associated markers in the recipient's spleen and not within the graft. These data suggest indeed that migration of donor DCs to secondary lymphoid organs is affected. We assume that HO-1 induction resulting in diminished alloreactivity after IRI is mediated by (a) decreased numbers and diminished antigenicity of DCs migrating to secondary lymphoid organs, (b) alleviated levels of presented allogeneic peptides to $CD8^+$ T cells due to the reduction of synthesized immunoproteasomes, and (c) affecting chemokines important for lymphocyte trafficking to secondary lymphoid organs, thus preventing efficient T-cell priming. Thus, donor pretreatment resulting in the inhibition of DC activation improves the outcome of marginal organ donors.

ACKNOWLEDGMENTS

Katja Kotsch was supported by a grant from the German Kidney Foundation and Else-Kröner Foundation. Paulo N. A. Martins was supported from the European Society of Organ Transplantation and the American Society of Transplantation. This work was partly supported by Deutsche Forschungsgemeinschaft (SFB 421, TP B2, and Tu 63/5-5). We thank Anke Jurisch for excellent technologic assistance. Drs. Tullius and Volk contributed equally as senior authors.

ABBREVIATIONS

CAN, chronic allograft nephropathy; CDH5, vascular endothelial-cadherin precursor CoPPIX, cobalt protoporphyrin-IX; CCR7, C-C motif receptor 7; DCs, dendritic cells; DGF, de-

layed graft function; HO-1, heme oxygenase 1; HSP, heat-shock protein; IFN-γ, interferon gamma; IκBa, I-kappa-B-alpha; IRI, ischemia/reperfusion injury; IP-10, interferon-inducible protein 10; LPS, lipopolysaccharide; MC, methylene chloride; PSMB8, proteasome component C13 precursor; PSMB9, proteasome chain 7 precursor; PSMB10, proteasome component MECL-1 precursor; PSME2, 11S proteasome regulator PA28 β subunit; STAT1, signal transducer and activator of transcription 1 a/β; TUBA1, tubulin α-1 chain.

REFERENCES

1. Ackerman AL and Cresswell P. Cellular mechanisms governing cross-presentation of exogenous antigens. *Nat Immunol* 5: 678–684, 2004.
2. Amberger A, Schneeberger S, Hernegger G, Brandacher G, Obrist P, Lackner P, Margreiter R, and Mark W. Gene expression profiling of prolonged cold ischemia and reperfusion in murine heart transplants. *Transplantation* 74: 1441–1449, 2002.
3. Amersi F, Buelow R, Kato H, Ke B, Coito AJ, Shen XD, Zhao D, Zaky J, Melinek J, Lassman CR, Kolls JK, Alam J, Ritter T, Volk HD, Farmer DG, Ghobrial RM, Busuttil RW, and Kupiec-Weglinski JW. Upregulation of heme oxygenase-1 protects genetically fat Zucker rat livers from ischemia/reperfusion injury. *J Clin Invest* 104: 1631–1639, 1999.
4. Araki M, Schenk AD, and Fairchild RL. Cytokines and chemokines: roles in the pathophysiology and therapy of ischemia and reperfusion injury. *Curr Opin Organ Transplant* 9: 139–144, 2004.
5. Barrett T, Suzek TO, Troup DB, Wilhite SE, Ngau WC, Ledoux P, Rudnev D, Lash AE, Fujibuchi W, and Edgar R. NCBI GEO: mining millions of expression profiles-database and tools. *Nucleic Acids Res* 1;33 Database Issue: D562–D62005, 2005.
6. Bonventre V and Zuk A. Ischemic acute renal failure: an inflammatory disease? *Kidney Int* 66: 480–485, 2004.
7. Bonventre JV. Mechanisms of ischemic acute renal failure. *Kidney Int* 43: 1160–78, 1993.
8. Bosio A, Knorr C, Janssen U, Gebel S, Haussmann HJ, and Muller T. Kinetics of gene expression profiling in Swiss 3T3 cells exposed to aqueous extracts of cigarette smoke. *Carcinogenesis* 23: 741–748, 2002.
9. Burne-Taney MJ, Kofler J, Yokota N, Weisfeldt M, Traystman RJ, and Rabb H. Acute renal failure after whole body ischemia is characterized by inflammation and T cell-mediated injury. *Am J Physiol Renal Physiol* 285: F87–F94, 2003.
10. Chapatte L, Ayyoub M, Morel S, Peitrequin AL, Levy N, Servis C, Van den Eynde BJ, Valmori D, and Levy F. Processing of tumor-associated antigen by the proteasomes of dendritic cells controls in vivo T-cell responses. *Cancer Res* 66: 5461–5468, 2006.
11. Chauveau C, Bouchet D, Roussel JC, Mathieu P, Braudeau C, Renaudin K, Tesson L, Soulillou JP, Iyer S, Buelow R, and Anegon I. Gene transfer of heme oxygenase-1 and carbon monoxide delivery inhibit chronic rejection. *Am J Transplant* 2: 581–592, 2002.
12. Chauveau C, Remy S, Royer PJ, Hill M, Tanguy-Royer S, Hubert FX, Tesson L, Brion R, Beriou G, Gregoire M, Josien R, Cuturi MC, and Anegon I. Heme oxygenase-1 expression inhibits dendritic cell maturation and proinflammatory function but conserves IL-10 expression. *Blood* 106: 1694–1702, 2005.
13. De Greef KE, Ysebaert DK, Ghielli M, Vercauteren S, Nouwen EJ, Eyskens EJ, and De Broe ME. Neutrophils and acute ischemia-reperfusion injury. *J Nephrol* 11: 110–122, 1998.
14. Edgar R, Domrachev M, and Lash AE. Gene expression omnibus: NCBI gene expression and hybridization array data repository *Nucleic Acids Res* 30: 207–210, 2002.
15. Eisen MB, Spellman PT, Brown PO, and Botstein D. Cluster analysis and display of genome-wide expression patterns. *Proc Natl Acad Sci U S A* 95: 14863–14868, 1998.
16. Gaczynska M, Goldberg AL, Tanaka K, Hendil KB, and Rock KL. Proteasome subunits X and Y alter peptidase activities in opposite ways to the interferon-gamma-induced subunits LMP2 and LMP7. *J Biol Chem* 271: 17275–17280, 1996.
17. Griffin TA, Nandi D, Cruz M, Fehling HJ, Kaer LV, Monaco JJ, and Colbert AA. Immunoproteasome assembly: cooperative incorporation of interferon gamma (IFN-gamma)-inducible subunits. *J Exp Med* 187: 97–104, 1998.
18. Groettrup M, Ruppert T, Kuehn L, Seeger M, Standera S, Koszinowski U, and Kloetzel PM. The interferon-gamma-inducible 11 S regulator (PA28) and the LMP2/LMP7 subunits govern the peptide production by the 20 S proteasome in vitro. *J Biol Chem* 270: 23808–23815, 1995.
19. Hancock WW, Buelow R, Sayegh MH, and Turka LA. Antibody-induced transplant arteriosclerosis is prevented by graft expression of anti-oxidant and anti-apoptotic genes. *Nat Med* 4: 1392–1396, 1998.
20. Hopken UE, Droese J, Li JP, Joergensen J, Breitfeld D, Zerwes HG, and Lipp, M. The chemokine receptor CCR7 controls lymph node-dependent cytotoxic T cell priming in alloimmune responses. *Eur J Immunol* 34: 461–470, 2004.
21. Katori M, Busuttil RW, and Kupiec-Weglinski JW. Heme oxygenase-1 system in organ transplantation. *Transplantation* 74: 905–912, 2002.
22. Kim BS, Lim SW, Li C, Kim JS, Sun BK, Ahn KO, Han SW, Kim J, and Yang CW. Ischemia-reperfusion injury activates innate immunity in rat kidneys. *Transplantation* 79: 1370–1377, 2005.
23. Koning OH, Ploeg RJ, van Bockel JH, Groenewegen M, van der Woude FJ, Persijn GG, and Hermans J. Risk factors for delayed graft function in cadaveric kidney transplantation: a prospective study of renal function and graft survival after preservation with University of Wisconsin solution in multi-organ donors: European Multicenter Study Group. *Transplantation* 63: 1620–1628, 1997.
24. Land WG. The role of postischemic reperfusion injury and other nonantigen-dependent inflammatory pathways in transplantation. *Transplantation* 79: 505–514, 2005.
25. Liano F and Pascual J. Epidemiology of acute renal failure: a prospective, multicenter, community-based study: Madrid Acute Renal Failure Study Group. *Kidney Int* 50: 811–818, 1996.
26. Macagno A, Kuehn L, de Giuli R, and Groettrup M. Pronounced up-regulation of the PA28alpha/beta proteasome regulator but little increase in the steady-state content of immunoproteasome during dendritic cell maturation. *Eur J Immunol* 31: 3271–3280, 2001.
27. Martins PNA, Pratschke J, Pascher A, Fritsche L, Frei U, Neuhaus P, and Tullius SG. Age and immune response in organ transplantation. *Transplantation* 79: 127–132, 2005.
28. Martins PN, Reutzel-Selke A, Jurisch A, Denecke C, Attrot K, Pascher A, Kotsch K, Pratschke J, Neuhaus P, Volk HD, and Tullius SG. Induction of carbon monoxide in donor animals prior to organ procurement reduces graft immunogenicity and inhibits chronic allograft dysfunction. *Transplantation* 82: 938–944, 2006.
29. Martins PN, Reuzel-Selke A, Jurisch A, Atrott K, Pascher A, Pratschke J, Buelow R, Neuhaus P, Volk HD, and Tullius SG. Induction of carbon monoxide in the donor reduces graft immunogenicity and chronic graft deterioration. *Transplant Proc* 37: 379–381, 2005.
30. Molitoris BA and Marrs J. The role of cell adhesion molecules in ischemic acute renal failure. *Am J Med* 106: 583–592, 1999.
31. Ojo AO, Wolfe RA, Held PJ, Port FK, and Schmouder RL. Delayed graft function: risk factors and implications for renal allograft survival. *Transplantation* 63: 968–974, 1997.
32. Otterbein LE, Soares MP, Yamashita K, and Bach FH. Heme oxygenase-1: unleashing the protective properties of heme. *Trends Immunol* 24: 449–455, 2003.
33. Otterbein LE, Kolls JK, Mantell LL, Cook JL, Alam J, and Choi AM. Exogenous administration of heme oxygenase-1 by gene transfer provides protection against hyperoxia-induced lung injury. *J Clin Invest* 103: 1047–1054, 1999.
34. Padovan E, Spagnoli GC, Ferrantini M, and Heberer M. IFN-alpha2a induces IP-10/CXCL10 and MIG/CXCL9 production in monocyte-derived dendritic cells and enhances their capacity to attract and stimulate CD8+ effector T cells. *J Leukoc Biol* 71: 669–676, 2002.
35. Palmowski MJ, Gileadi U, Salio M, Gallimore A, Millrain M, James E, Addey C, Scott D, Dyson J, Simpson E, and Cerundolo V. Role of immunoproteasomes in cross-presentation. *J Immunol* 177: 983–990, 2006.
36. Pratschke J, Paz D, Wilhelm MJ, Laskowski I, Kofla G, Vergopoulos A, MacKenzie HJ, Tullius SG, Neuhaus P, Hancock WW,

Volk HD, and Tilney NL. Donor hypertension increases graft immunogenicity and intensifies chronic changes in long-surviving renal allografts. *Transplantation* 77: 43–48, 2004.
37. Pratschke J, Tullius SG, and Neuhaus P. Brain death associated ischemia/reperfusion injury. *Ann Transplant* 9: 78–80, 2004.
38. Ryter SW, Alam J, and Choi AM. Heme oxygenase-1/carbon monoxide: from basic science to therapeutic applications. *Physiol Rev* 86: 583–650, 2006.
39. Schwarz K, Eggers M, Soza A, Koszinowski UH, Kloetzel PM, and Groettrup M. The proteasome regulator PA28alpha/beta can enhance antigen presentation without affecting 20S proteasome subunit composition. *Eur J Immunol* 30: 3672–3679, 2000.
40. Seiler M, Brabcova I, Viklicky O, Hribova P, Rosenberger C, Pratschke J, Lodererova A, Matz M, Schonemann C, Reinke P, Volk HD, and Kotsch K. Heightened expression of the cytotoxicity receptor NKG2D correlates with acute and chronic nephropathy after kidney transplantation. *Am J Transplant* 72: 423–433, 2007.
41. Sijts AJ, Ruppert T, Rehermann B, Schmidt M, Koszinowski U, and Kloetzel PM. Efficient generation of a hepatitis B virus cytotoxic T lymphocyte epitope requires the structural features of immunoproteasomes. *J Exp Med* 191: 503–514, 2000.
42. Singbartl K and Ley K. Protection from ischemia-reperfusion induced severe acute renal failure by blocking E-selectin. *Crit Care Med* 28: 2507–2514, 2000.
43. Stegall MD, Park WD, Kim DY, Covarrubias M, Khair A, and Kremers WK. Changes in intragraft gene expression secondary to ischemia reperfusion after cardiac transplantation. *Transplantation* 74: 924–930, 2002.
44. Strehl B, Joeris T, Rieger M, Visekruna A, Textoris-Taube K, Kaufmann SH, Kloetzel PM, Kuckelkorn U, and Steinhoff U. Immunoproteasomes are essential for clearance of *Listeria monocytogenes* in nonlymphoid tissues but not for induction of bacteria-specific CD8+ T cells. *J Immunol* 177: 6238–6244, 2006.
45. Supavekin S, Zhang W, Kucherlapati R, Kaskel FJ, Moore LC, and Devarajan P. Differential gene expression following early renal ischemia/reperfusion. *Kidney Int* 63: 1714–1724, 2003.
46. Tenhunen R, Marver HS, and Schmid R. The enzymatic conversion of heme to bilirubin by microsomal heme oxygenase. *Proc Natl Acad Sci U S A* 61: 748–755, 1968.
47. Tsuchihashi S, Zhai Y, Fondevila C, Busuttil RW, and Kupiec-Weglinski JW. HO-1 upregulation suppresses type 1 IFN pathway in hepatic ischemia/reperfusion injury. *Transplant Proc* 37: 1677–1678, 2005.
48. Tullius SG, Nieminen-Kelha M, Buelow R, Reutzel-Selke A, Martins PN, Pratschke J, Bachmann U, Lehmann M, Southard D, Iyer S, Schmidbauer G, Sawitzki B, Reinke P, Neuhaus P, and Volk HD. Inhibition of ischemia/reperfusion injury and chronic graft deterioration by a single-donor treatment with cobalt-protoporphyrin for the induction of heme oxygenase-1. *Transplantation* 74: 591–598, 2002.
49. Wiesel P, Patel AP, DiFonzo N, Marria PB,. Sim CU, Pellacani A, Maemura K, LeBlanc BW, Marino K, Doerschuk CM, Yet SF, Lee ME, and Perrella MA. Endotoxin-induced mortality is related to increased oxidative stress and end-organ dysfunction, not refractory hypotension, in heme oxygenase-1-deficient mice. *Circulation* 102: 3015–3022, 2000.
50. Yoshida T, Kurella M, Beato F, Min. H, Ingelfinger JR, Stears RL, Swingford RD, Gullans SR, and Tabg SS. Monitoring changes in gene expression in renal ischemia-reperfusion in the rat. *Kidney Int* 61: 1646–1654, 2002.
51. Zhai Y, Shen XD, Hancock WW, Gao F, Qiao B, Lassman C, Belperio JA, Strieter RM, Busuttil RW, and Kupiec-Weglinski JW. CXCR3+CD4+ T cells mediate innate immune function in the pathophysiology of liver ischemia/reperfusion injury. *J Immunol* 176: 6313–6322, 2006.

Address reprint requests to:
Katja Kotsch, Ph.D.
Institute of Medical Immunology
Universitätsmedizin Berlin Charité, Campus Mitte
Charitéplatz 1
D-10117 Berlin, Germany

E-mail: katja.kotsch@charite.de

Date of first submission to ARS Central, June 24, 2007; date of acceptance, July 1, 2007.

This article has been cited by:

1. A. Siedlecki, W. Irish, D. C. Brennan. 2011. Delayed Graft Function in the Kidney Transplant. *American Journal of Transplantation* no-no. [CrossRef]
2. Yoshiaki Hara, Meaghan Stolk, Jochen Ringe, Tilo Dehne, Juliane Ladhoff, Katja Kotsch, Anja Reutzel-Selke, Petra Reinke, Hans-Dieter Volk, Martina Seifert. 2011. In vivo effect of bone marrow-derived mesenchymal stem cells in a rat kidney transplantation model with prolonged cold ischemia. *Transplant International* no-no. [CrossRef]
3. Nicolas Chatauret, Raphael Thuillier, Thierry Hauet. 2011. Preservation strategies to reduce ischemic injury in kidney transplantation: pharmacological and genetic approaches. *Current Opinion in Organ Transplantation* **16**:2, 180-187. [CrossRef]
4. Robert Öllinger, Johann Pratschke. 2010. Role of heme oxygenase-1 in transplantation. *Transplant International* **23**:11, 1071-1081. [CrossRef]
5. Katja Kotsch, Kristina Kunert, Vera Merk, Anja Reutzel-Selke, Andreas Pascher, Florian Fritzsche, Stefan G. Tullius, Johann Pratschke. 2010. Novel Markers in Zero-Hour Kidney Biopsies Indicate Graft Quality and Clinical Outcome. *Transplantation* **90**:9, 958-965. [CrossRef]
6. Dong Jun Park, Anupam Agarwal, James F. George. 2010. Heme Oxygenase-1 Expression in Murine Dendritic Cell Subpopulations. *The American Journal of Pathology* **176**:6, 2831-2839. [CrossRef]
7. Csaba SzaboMedicinal Chemistry and Therapeutic Applications of the Gasotransmitters NO, CO, and H 2 S and their Prodrugs . [CrossRef]
8. Bo Chen, Lingling Guo, Chunlan Fan, Subhashini Bolisetty, Reny Joseph, Marcienne M. Wright, Anupam Agarwal, James F. George. 2009. Carbon Monoxide Rescues Heme Oxygenase-1-Deficient Mice from Arterial Thrombosis in Allogeneic Aortic Transplantation. *The American Journal of Pathology* **175**:1, 422-429. [CrossRef]
9. Jozef Dulak . 2007. Changing Faces of Heme Oxygenases. *Antioxidants & Redox Signaling* **9**:12, 2043-2048. [Citation] [PDF] [PDF Plus]